

New hexagonal perovskite with Mn⁴⁺ and Mn⁵⁺ at distinct structural positions

This content has been downloaded from IOPscience. Please scroll down to see the full text.

2015 J. Phys.: Conf. Ser. 644 012004

(<http://iopscience.iop.org/1742-6596/644/1/012004>)

View [the table of contents for this issue](#), or go to the [journal homepage](#) for more

Download details:

IP Address: 161.23.96.94

This content was downloaded on 25/04/2016 at 11:36

Please note that [terms and conditions apply](#).

New hexagonal perovskite with Mn⁴⁺ and Mn⁵⁺ at distinct structural positions

N V Tarakina^{1,2}, A P Tyutyunnik³, G V Bazuev³, A D Vasiliev^{4,5}, I F Berger³,
C Gould², I V Nikolaenko³

¹The NanoVision Centre, School of Engineering and Materials Science, Queen Mary University of London, Mile End, London E1 4NS, United Kingdom

²Experimentelle Physik III, Physikalisches Institut and Wilhelm Conrad Röntgen - Research Centre for Complex Material Systems, Universität Würzburg, Am Hubland, D-97074 Würzburg, Germany

³Institute of Solid State Chemistry, Ural Branch of the Russian Academy of Sciences, 91 Pervomayskaya, 620990, Ekaterinburg, Russia

⁴L.V. Kirensky Institute of Physics, Siberian Branch of Russian Academy of Sciences, 50 Akademgorodok, 660036, Krasnoyarsk, Russia

⁵Siberian Federal University, Svobodny pr. 79, 660041 Krasnoyarsk, Russia

E-mail: n.tarakina@qmul.ac.uk

Abstract. A new hexagonal perovskite, Ba₇Li_{1.75}Mn_{3.5}O_{15.75}, has been synthesised using microwave-assisted solid-state synthesis. Its crystal structure has elements typical for the layered hexagonal perovskites and quasi-one-dimensional oxides, hence representing a new polytype. Structural solution based on simultaneous refinement of X-ray and neutron diffraction data shows that Ba₇Li_{1.75}Mn_{3.5}O_{15.75} crystallizes in a hexagonal unit cell with parameters $a = 5.66274(2)$ Å and $c = 16.7467(1)$ Å ($V = 465.063(4)$ Å³). Columns of face-shared octahedra occupied by Mn⁴⁺, Li⁺ cations and vacancies along the c axis are separated in the ab plane by barium atoms, so that every sixth layer, the coordination of Mn⁵⁺ and Li⁺ changes to tetrahedral. Separation of Mn⁴⁺ and Mn⁵⁺ cations in two distinct structural positions makes the structure unique. A scanning transmission electron microscopy study revealed the formation of a rhombohedrally centered supercell, which might be attributed to the ordering of manganese and lithium atoms among cationic sites.

1. Introduction

AMnO₃ (A = alkali-earth element) perovskites display a variety of interesting magnetic and electronic phenomena (metallic ferromagnetism, charge or orbital ordering, etc.), which result from competing charge, exchange and phonon interactions [1]. A fine-tuning of these competing interactions and thus control of the functional properties of these materials can be realized by substituting either A-site cations or Mn with other cations (of different sizes/charges). Substitution changes the distribution of the charges (ratio between Mn cations in different oxidation states) or leads to the formation of different polymorphs (changing the ratio of corner-sharing (cubic) to face-sharing (hexagonal) perovskite layers within one structure): 6H-Ba_{0.7}Sr_{0.3}Ru_{1-x}Mn_xO₃ ($0.2 \leq x \leq 0.4$) [2], 8H-Ba₈Ta₆NiO₂₄ [3],



10H-Ba₅Sn_{1.1}Mn_{3.9}O₁₅ [4], 12H-(BaSr)_{0.5}Mn₄Cr₂O₁₇ [5], 9R-BaRu_{1-x}Mn_xO₃ (0≤x≤0.90) [6], 12R-Ba₃NdMn₂O₉ [7], 16R-Ba₄Ca_{1-x}Mn_{1+x}O_{12-δ} [8], etc. — see Figure. 1.

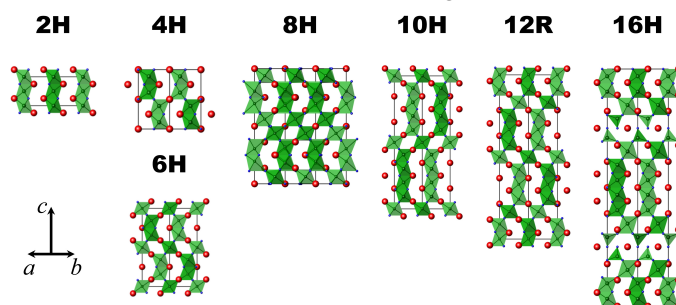


Figure 1. Crystal structures of some polytypes of BaMnO₃ and different polymorphs obtained by substitution of Mn by other elements (A'). Red and blue spheres indicate Ba and oxygen sites, respectively. Positions indicated by green polyhedra are occupied by manganese and A' atoms.

Substitution of the Mn⁴⁺ ions in BaMnO₃ by cations of elements with smaller valence leads to the formation of compounds with mixed or enhanced average degree of oxidation of manganese such as the new family of layered structures of the general formula Ba_{5+n}Ca₂Mn_{3+n}O_{3n+14}, the hexagonal 6-layer perovskite Ba₃ErMn₂O₉ [9], as well as the quasi-one-dimensional compounds Ba₄NaMn₂O₉ [10] and Sr₄LiMn₂O₉ [11]. A structure with distinct atomic positions for the manganese Mn⁴⁺ and Mn⁵⁺ ions has been found for Ba₇Ca₂Mn₅O₂₀ but not for the aforementioned quasi-one-dimensional oxides. In this work, we focused on synthesis, crystal structure and magnetic properties of the new Ba₇Li_{1.75}Mn_{3.5}O_{15.75} oxide.

2. Results and Discussion

Ba₇Li_{1.75}Mn_{3.5}O_{15.75} was been synthesized for the first time, by means of a microwave-assisted solid-state method. A stoichiometric mixture of the initial reagents BaCO₃ (99.9%), Li₂CO₃ (99.99%) and MnO₂ (99.9%) was calcined at 950°C for 1 hour in a microwave furnace (generator power of 700 W and frequency of 2450 MHz), then ground, pressed into a pellet and annealed at 1030°C for 2 hours with intermediate grinding after 1 hour of annealing.

Table 1. Atomic coordinates and isotropic thermal parameters ($U_{\text{iso}} \times 100, \text{\AA}^2$) for Ba₇Li_{1.75}Mn_{3.5}O_{15.75}.

Atom	Site [§]	x/a	y/b	z/c	Fraction	$U_{\text{iso}} \times 100$
Ba(1)	1a	0.0	0.0	0.0	1.0	3.6(1)
Ba(2)	2d	1/3	2/3	0.5724(2)	1.0	2.63(9)
Ba(3)	2d	2/3	1/3	0.6964(2)	1.0	2.3(1)
Ba(4)	2d	1/3	2/3	0.8263(1)	1.0	1.9(1)
Mn/Li(1)	2c	0.0	0.0	0.3509(4)	0.79/0.21(1)	3.9(2)*
Mn/Li(2)	1b	0.0	0.0	1/2	0.67/0.33(1)	3.9(2)*
Mn/Li(3)	2d	2/3	1/3	0.9085(6)	0.80/0.20(1)	3.9(2)*
Mn/Li(4)	2c	0.0	0.0	0.194(2)	0.005/0.995(8)	3.9(2)*
O(1)	6i	0.1785(8)	0.8215(8)	0.1307(4)	0.88(1)	1.73(8)*
O(2)	6i	0.8443(8)	0.689(2)	0.5677(5)	0.718(8)	1.73(8)*
O(3)	6i	0.1511(7)	0.302(1)	0.7083(4)	1.0	1.73(8)*
O(4)	2d	2/3	1/3	0.004(1)	0.59(2)	1.73(8)*

[§]Symmetry multiplicity and Wyckoff symbol; *Thermal parameters of manganese/lithium and oxygen atoms were constrained as single variables.

X-ray and neutron powder diffraction patterns were indexed in a hexagonal unit cell with parameters $a = 5.66274(2)$ Å and $c = 16.7467(1)$ Å. No systematic absences were observed, so all primitive trigonal space groups can be chosen. A crystal structure similar to the structure of the quasi-1D $\text{Sr}_4\text{LiMn}_2\text{O}_9$ oxide, but with positions of one alkali-earth atom and one Mn atom, exchanged (Figure 2, a,b) was used as a starting model. In the final model, columns of face-sharing octahedra occupied by Mn^{4+} and Li^+ oriented along the c axis are cut in short chains of five by Ba atoms, while in the barium columns every sixth layer is now occupied by $\text{Mn}^{5+}/\text{Li}^+$ in tetrahedral coordination. For the resulting model the $P-3m1$ (164) space group was chosen. To get more accurate positions of the lithium and the oxygen atoms, the neutron (ND) and X-ray diffraction (XRD) data were refined simultaneously (Table 1). The presence of the structural elements described above was confirmed by high-resolution transmission electron microscopy; however, selected-area electron diffraction (SAED) patterns showed the formation of a rhombohedrally centered supercell with unit cell parameters $a = 10$ Å, $c = 51.3$ Å. Extinction conditions point to five possible space groups: $R3$ (146), $R-3$ (148), $R32$ (155), $R3m$ (160), $R-3m$ (166), Figure 2, e-g. An analysis of the intensity distributions on high-angle annular dark field scanning transmission electron microscopy (HAADF-STEM) images suggests that the formation of a supercell is related to additional ordering of Mn and Li atoms in the ab plane (Figure 2, c,d). In particular, according to the structural model obtained from XRD all atomic columns along the $[1-10]_{P-3m1}$ ($[100]_{R-3m}$) direction should give equal contrast on the HAADF-STEM images, however on the recorded images two columns of higher intensity alternate with one column of lower intensity, Figure 2 (h, i). Simulations of HAADF-STEM images did not provide an unambiguous solution of the cation distribution; additional annular bright-field imaging or atomic-column resolved Li-K edge spectrum imaging are required to obtain a full description of the supercell. Here and in the following we will refer to such a set of three columns as one block. The described cation ordering explains the increase of the a parameter of the unit cell by a factor of $\sqrt{3}$ and a rotation of the crystal axes by 30° with respect to the primitive trigonal lattice.

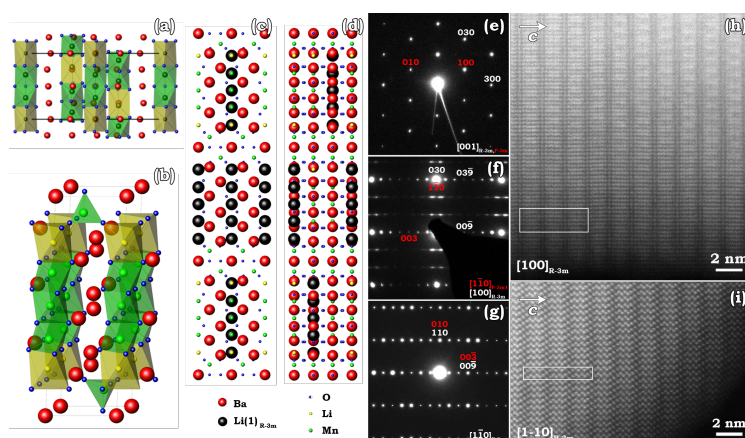


Figure 2. Schematic drawings of quasi-one-dimensional $\text{Ba}_4\text{NaMn}_2\text{O}_9$ oxide (a), the average structure of $\text{Ba}_7\text{Li}_{1.75}\text{Mn}_{3.5}\text{O}_{15.75}$ obtained from XRD (b), the rhombohedral superstructure of $\text{Ba}_7\text{Li}_{1.75}\text{Mn}_{3.5}\text{O}_{15.75}$ in projections on $(110)_{R-3m}$ (c), $(1-10)_{R-3m}$ (d). SAED patterns taken along the main zone axis (e-g). HAADF-STEM images taken along $[100]_{R-3m}$ (h) and $[1-10]_{R-3m}$ (i) directions.

A periodic stacking of blocks along the c direction with shifts equal to $2/3$ of the width of the block would result in a perfect rhombohedral supercell. However, occasional shifts over $1/3$ ($= -2/3$) have been observed in the HAADF-STEM images, destroying the perfect rhombohedral symmetry of the crystal and causing the presence of diffuse streaks in the SAED patterns along the $[100]_{R-3m}$ direction as well as problems with refining XRD and ND data using the supercell model. The defect structure can be described either through the formation of twin planes perpendicular to the c direction or through stacking faults along the c direction.

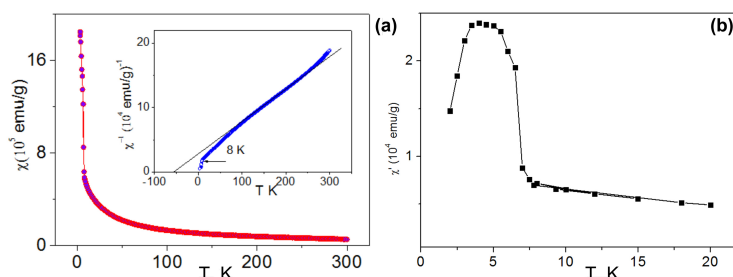


Figure 3. Temperature dependence of the DC magnetic susceptibility χ (a) and of the real component of the AC magnetic susceptibility χ' for $\text{Ba}_7\text{Li}_{1.75}\text{Mn}_{3.5}\text{O}_{15.75}$. The inset shows the $\chi^{-1}(T)$ dependence.

Static magnetic susceptibility measurements were carried out at $H = 0.3$ kOe in the temperature range 3-300 K (Figure 3). Between 100 and 220 K the magnetic susceptibility χ obeys the Curie-Weiss law $\chi = C/(T-\theta)$, where C is the Curie constant ($2.40 \text{ cm}^3 \text{ K/mol}$), and θ is the Weiss temperature ($\theta = -55 \text{ K}$). Above 220 K and below 100 K, deviations from a straight-line behavior are observed, pointing to an antiferromagnetic exchange interaction between the paramagnetic manganese ions in $\text{Ba}_7\text{Li}_{1.75}\text{Mn}_{3.5}\text{O}_{15.75}$, similar to those found in the $\text{Sr}_4\text{AMn}_2\text{O}_9$ series ($A = \text{Li, Zn, Ni, Cu}$) [11-13]. For the determination of the reason of the sharp χ increase below 8 K, AC magnetic susceptibility measurements were performed. The real χ' and imaginary χ'' components of the magnetic susceptibility were determined for alternating-magnetic-field amplitudes of up to 4 Oe at a frequency of $f = 80$ Hz and temperatures in the range $T = 2 - 20$ K (Fig. 3). Below 8 K, χ' increases (just like χ), until it reaches a maximum at 5 K, below which it decreases. The occurrence of a maximum in the dependence of χ' on T is a signature of a magnetic transition, the nature of which is possibly related to antiferromagnetic properties below the transition temperature.

3. Conclusions

$\text{Ba}_7\text{Li}_{1.75}\text{Mn}_{3.5}\text{O}_{15.75}$ represents a new hexagonal perovskite polytype with structural elements typical for layered hexagonal perovskites and the quasi-one-dimensional oxides, and with Mn^{4+} and Mn^{5+} cations distinctly distributed between structural positions. The temperature dependence of the magnetic susceptibility reveals the presence of antiferromagnetic exchange interactions between the paramagnetic manganese ions in the hexagonal columns and suggests antiferromagnetic order < 5 K.

4. Acknowledgments

X-ray powder diffraction studies were carried out at the Center for collective use "X-ray structure analysis" at the Institute of Solid State Chemistry, UrB RAS (Ekaterinburg, Russia).

References

- [1] Tokura Y and Nagaosa N 2000 *Science* **288** 462
- [2] Yin C, Li G, Lin J and Attfield J P 2009 *Chem. Asian J.* **4** 969
- [3] Shpanchenko R V, Nistor L, Van Tendeloo G *et al* 1995 *J. Solid State Chem.* **114** 560
- [4] Yin C, Li G, Jin T, Tao J, Richardson J, Loong C-K *et al* 2010 *J. Alloys Compounds* **489** 152
- [5] Clark J H and Hayward M A 2008 *Chem. Mater.* **20** 4612
- [6] Yin C, Li G, Kockelmann W A, Lin J and Attfield J P 2009 *Phys. Rev. B* **80** 094420
- [7] Yang H, Tang Y K, Yao L D, Zhang W, Li Q A *et al* 2007 *J. Alloys Compounds* **432** 283
- [8] Floros N, Michel C, Hervieu M and Raveau B 2000 *Chem. Mater.* **12** 3197
- [9] Rabbow C and Müller-Buschbaum H Z 1994 *Naturforsch.* **498** 1277
- [10] Quarez E, Roussel P L, Pérez O, Leligny H *et al* 2004 *Solid State Sci.* **6** 631
- [11] Bazuev G V, Tyutyunnik A P, Berger I F *et al* 2011 *J. Alloys Compounds* **509** 6158
- [12] Bazuev G V, Krasilnikov N V and Kellerman D G 2003 *J. Alloys Compounds* **352**, 190
- [13] Abed A El, Gaudin E, Darriet J and Whangbo M-H 2002 *J. Solid State Chem.* **163**, 513